AD-A061 042 ALASKA UNIV FAIRBANKS GEOPHYSICAL INST F/G 4/1
ORIGIN OF THE AURORAL ELECTRIC FIELD.(U)
DEC 77 J R KAN, S I AKASOFU F19628-77-C-0038
UNCLASSIFIED AFGL-TR-78-0018 NL

1 OF 1
AD A061 042

END
DATE FILMED
2-79
DDC

LEVEL II

AFGL-TR-78-0018

ORIGIN OF THE AURORAL ELECTRIC FIELD

J.R. Kan
S.-I. Akasofu

Geophysical Institute
University of Alaska
Fairbanks, Alaska 99701

Final Report
September, 1976 - September, 1977

December, 1977

Approved for public release; distribution unlimited

AIR FORCE GEOPHYSICS LABORATORY
AIR FORCE SYSTEMS COMMAND
UNITED STATES AIR FORCE
HANSCOM AFB, MASSACHUSETTS 01731

Unclassified

SECURITY CLASSIFICATION OF THIS PAGE (When Data Entered)

(19) REPORT DOCUMENTATION PAGE	READ INSTRUCTIONS BEFORE COMPLETING FORM
(18) 1. REPORT NUMBER AFGL-TR-78-0018	2. GOVT ACCESSION NO. 3. RECIPIENT'S CATALOG NUMBER
(6) 4. TITLE (and Subtitle) ORIGIN OF THE AURORAL ELECTRIC FIELD.	(9) 5. TYPE OF REPORT & PERIOD COVERED Final Report. Sep 76-Sep 77
	6. PERFORMING ORG. REPORT NUMBER
(10) 7. AUTHOR(s) J.R. Kan S.-I. Akasofu	(15) 8. CONTRACT OR GRANT NUMBER(s) F19628-77-C-0038, NSF-ATM77-11371
9. PERFORMING ORGANIZATION NAME AND ADDRESS Geophysical Institute University of Alaska Fairbanks, Alaska 99701	10. PROGRAM ELEMENT, PROJECT, TASK AREA & WORK UNIT NUMBERS 61102F (16) 2311 G2 02 (17) G2
11. CONTROLLING OFFICE NAME AND ADDRESS Air Force Geophysics Laboratory Hanscom AFB, Massachusetts 01731 Monitor/ Michael Smiddy/PHR	(11) 12. REPORT DATE Dec 1977 13. NUMBER OF PAGES 30
14. MONITORING AGENCY NAME & ADDRESS(if different from Controlling Office) (12) 32p.	15. SECURITY CLASS. (of this report) Unclassified
	15a. DECLASSIFICATION/DOWNGRADING SCHEDULE

16. DISTRIBUTION STATEMENT (of this Report)

Approved for public release; distribution unlimited

17. DISTRIBUTION STATEMENT (of the abstract entered in Block 20, if different from Report)

18. SUPPLEMENTARY NOTES

19. KEY WORDS (Continue on reverse side if necessary and identify by block number)

Aurora, Electric Fields, Field-Aligned Currents, Particle Accelerations

20. ABSTRACT (Continue on reverse side if necessary and identify by block number)

A theory is presented to show that a pair of electric fields directed towards each other and perpendicular to the current sheet is inherent to electron current sheets in dynamic equilibrium. The theory predicts self-consistently the magnitude of the electric field and the width of the current sheet for a given current density and the ion and electron energy densities. It is also shown that the potential difference associated with the inherent electric fields is on the order of the ion thermal →

DD FORM 1 JAN 73 1473 EDITION OF 1 NOV 65 IS OBSOLETE S/N 0102 LF 014 6601

SECURITY CLASSIFICATION OF THIS PAGE (When Data Entered)

152 450

energy and that this potential difference must be distributed almost entirely along field lines between the plasma sheet and the ionosphere as a result of closing the auroral sheet current through the ionosphere. Thus, one can make a few important observable predictions, such as the relationship between the width and the brightness of an auroral arc, and the average energy of auroral electrons as a function of latitudes. These predictions are qualitatively supported by observations.

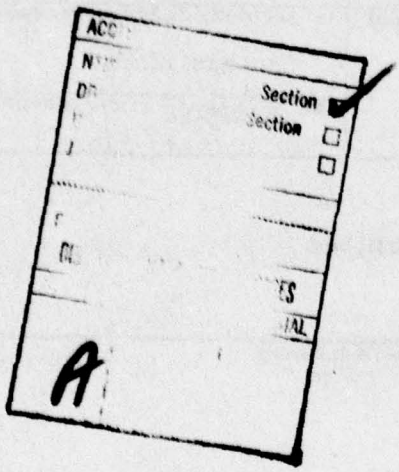

1. Introduction

Observations of intense perpendicular dc electric fields up to about one V/m, reported by Burch et al. (1976), Wescott et al., (1976) and Mozer et al. (1977) have opened a new era in auroral research. These electric fields are confined in a layer of a few tens of kilometers in latitudinal thickness and may well be magnetically connected to discrete auroral forms (Davis, 1978). The electric fields are in pairs, pointing towards each other, and are predominantly perpendicular to the magnetic field lines. There are still two possibilities in the distribution of the field-aligned component of the electric field. One is that the parallel electric field of order 1 mV/m is distributed over a distance of a few thousand kilometers, and the other is that the total potential drop is confined in a relatively short distance, say, less than 100 km.

In an attempt to understand the origin of this electric field distribution, one has at least two choices:

(i) The parallel electric field along the field lines, either distributed or localized, is the primary field and the pair of perpendicular electric field components (of magnitude 1 V/m) arises as a consequence of particular boundary conditions.

(ii) The pair of perpendicular electric fields is the primary field and the parallel electric field component arises as a consequence of particular boundary conditions.

It may be said that most of the ideas proposed so far on the origin of the electric field for the acceleration of auroral particles belong naturally to the first group. The double layer model proposed by Block

(1972, 1975), Alfvén (1977) and Fälthammar (1977), is an example. Lennartsson (1976) considered magnetic mirroring of downflowing hot electrons as a cause of the parallel electric field. Kan (1975) and Kan and Akasofu (1976) considered an electric field which is associated with a plasma flow into a converging magnetic field configuration. Various instabilities have also been suggested to produce a potential drop along field lines (Kindel and Kennel, 1971; Papadopoulos, 1977; Hudson et al., 1978).

The purpose of this paper is to explore the second possibility. In particular we shall show that a pair of the intense electric fields is inherent to the current sheet and that the parallel electric field component along auroral field lines is a natural consequence of magnetosphere-ionosphere coupling via the auroral sheet current.

The physical mechanism for this inherent electric field of a current sheet can be understood as follows. Consider a high-β plasma (β = plasma pressure/magnetic pressure) in which electrons carry an electric current along a convergent external magnetic field. The ions are in thermal motion but are assumed to carry no current for simplicity. The magnetic force due to the current is acting only on the current-carrying electrons. Thus, the electron gas is confined by the self-magnetic field via the so-called 'current pinch.' The ion gas is free from the current pinch and, therefore, tends to undergo thermal expansion in the high-β plasma region. As the ion gas expands, charge separation takes place because the electron gas is magnetically confined and cannot follow the ion motion. The electric field resulting from the charge separation tends to limit the extent of the ion gas expansion. When the

current sheet reaches dynamic equilibrium, the electron gas is confined by the self-magnetic force while the ion gas is confined mainly by the electric force. Note that the electric field will be directed towards the center plane of the current sheet as long as the electrons are the dominant current carrier. The net force density is zero everywhere throughout the current sheet. For convenience, this type of current sheet equilibrium will hereafter be called non-neutral current sheet equilibrium. The same physical argument can be made to a current sheet in which the ion gas is carrying a fraction of the current. As long as the magnetic force is insufficient for confining the ion gas, the current sheet will be non-neutral. A quantitative formulation of the non-neutral current sheet equilibria is given in the next section in which we show that the observed pair of electric fields is an inherent property of the non-neutral current sheet. In this connection, it should be mentioned that Swift (1976) presented a V-shaped equipotential model in which the total potential difference is assumed given rather than self-determined. Moreover, the width of the model is restricted to a few ion gyroradius due to the combined use of the guiding center approximation and the quasi-neutral approximation. In the present paper, the total potential difference and several other crucial quantities of the sheet current are self-consistently determined.

The inherent electric field of the current sheet can be treated as the upper boundary condition imposed on the acceleration region. Since we use plasma parameters in the plasma sheet to determine the current sheet characteristics, the upper boundary can be considered to be located in the plasma sheet at a few earth radii altitude. The lower boundary

condition is determined by the ionosphere. We shall show that the Pederson conductivity even in an undisturbed ionosphere is high enough to drive the Pederson current by an ionospheric electric field which is much smaller than the inherent electric field of the auroral current sheet. Thus, almost the entire potential difference associated with the inherent electric field must be dropped between the plasma sheet and the ionosphere. As a result, there will be an upward electric field along the field lines which accelerates the current-carrying auroral electrons.

Although the potential distribution along field lines between the plasma sheet and the ionosphere has yet to be worked out, the proposed theory can make several predictions, because most of the observable effects are determined by the upper and/or lower boundary conditions, rather than conditions in the intermediate regions. We shall show that those predictions are in qualitative agreement with available observations.

2. Non-neutral Current Sheet Equilibria and the Perpendicular Electric Field

In this section, a class of non-neutral current sheet equilibria will be studied to show that a pair of electric fields pointing toward each other is an inherent property of a current sheet in dynamic equilibrium.

The external field lines will be assumed straight and converging uniformly along the z' axis in a rectangular Cartesian coordinate system (x', y', z'). We now introduce a coordinate system in which z measures the distance along field lines, and x and y are defined by the conservation of magnetic flux, i.e.,

$$x = (B/B_0)^{\frac{1}{2}} x'$$
$$y = (B/B_0)^{\frac{1}{2}} y' \qquad (1)$$

It is seen that x and y are constant along a field line. For a slowly convergent field, such as the earth's dipole, $z \cong z'$. From the conservation of particle flux, it can be shown that the number density n of a current-carrying species measured in the unprimed coordinate system is related to n′ in the primed coordinate system by $n = (B_0/B)n'$. For convenience, our discussion will be carried out in the unprimed coordinate system in which field lines are parallel to the z axis.

The current sheet will be assumed one-dimensional depending only on the x axis. The current is flowing along the external field lines parallel to the z axis. The relevant constants are the Hamiltonian and the z component of the canonical momentum given by

$$H = \frac{1}{2} m (v_x^2 + v_y^2 + v_z^2) + q\phi(x) \qquad (2)$$

$$P_z = mv_z + (q/c)A_z(x) \qquad (3)$$

where q and m are the charge and mass of the particle, respectively, $\phi(x)$ is the electrostatic potential and $A_z(x)$ is the z component of the magnetic potential.

Any function of constants of the motion is a solution to the Vlasov equation,

$$\frac{\partial f}{\partial t} + \vec{v} \cdot \frac{\partial f}{\partial \vec{x}} + q(\vec{E} + \vec{v} \times \vec{B}) \cdot \frac{\partial f}{\partial \vec{v}} = 0 \qquad (4)$$

which is the governing equation for the dynamics of a collisionless plasma. This general result is a statement of the Liouville theorem (e.g., Longmire, 1963). As a first approximation, we choose to consider a simple plasma model in which both the electrons and ions are assumed monoenergetic and may stream along the z axis. The simplicity of this plasma model is particularly suited for illustrating the underlying physics of the non-neutral current sheet equilibrium. Since the current is assumed to flow entirely in the z direction, only the z component of the canonical momentum is required to appear in the distribution function. Thus, the distribution function for the monoenergetic plasma can be written as

$$f_s = \frac{N_s}{\pi} \delta\left(\frac{H_s - \varepsilon_s}{m_s/2}\right) \delta\left(\frac{P_{zs}}{m_s} - V_s\right) \qquad (5)$$

where the subscript s denotes the species, and ε_s and V_s are the total energy and the streaming speed at locations where ϕ and A vanish; H_s and P_{zs} are given in (1) and (3) respectively. This type of monoenergetic plasma model has been used to describe relativistic electron beam equilibria in fusion research (e.g. Hammer and Rostoker, 1970; Kan and Lai, 1972).

Note that the external magnetic field parallel to the current can be added to or removed from the equilibrium current sheet without any effect on the dynamic equilibrium simply because the external field is parallel to the current. Similarly, a uniform magnetized plasma can be

added to the current sheet as the background plasma without affecting the pressure balance condition.

The number density, given by the zeroth moment of the distribution function, can be written as

$$n_s = N_s \int_0^\infty dv_\perp^2 \int_{-\infty}^{\infty} dv_{||}\, \delta\left(v_\perp^2 + v_{||}^2 + \frac{2q_s\phi}{m_s} - \frac{2\varepsilon_s}{m_s}\right) \delta\left(v_{||} + \frac{q_s A}{m_s c} - V_s\right)$$

$$= N_s \int_0^\infty dv_\perp^2\, \delta\left[v_\perp^2 + \left(V_s - \frac{q_s A}{m_s c}\right)^2 + \frac{2q_s\phi}{m_s} - \frac{2\varepsilon_s}{m_s}\right]$$

$$= \begin{cases} N_s & |x| \le \ell_s \\ 0 & |x| > \ell_s \end{cases} \qquad (6)$$

where ℓ_s is the location of the boundary of each species of the current sheet and is defined by

$$\frac{\varepsilon_s - q_s\,\phi(\ell_s)}{\frac{1}{2}m_s\left(V_s - q_s A(\ell_s)/m_s c\right)^2} = 1 \qquad (7)$$

Thus, in this model the number density is constant (N_s) within the layer (of thickness ℓ_s) for each species. Note that the subscript z on A(x) has been dropped since only the z component of the magnetic potential appears in this model. It should also be noted that the LHS of (7) is greater than unity for $|x| < \ell_s$ and less than unity for $|x| > \ell_s$.

The particle flux, given by the first moment of the distribution function, can be written as

$$n_s\langle v_{||}\rangle = \int v_{||} f d^3v$$

$$= \begin{cases} N_s\left(V_s - \frac{q_s A}{m_s c}\right) & |x| \le \ell_s \\ 0 & |x| < \ell_s \end{cases} \qquad (8)$$

where ℓ_s is again defined by (7).

The self-consistent electric and magnetic fields of the current sheet in dynamic equilibrium are given by the solutions of the Maxwell equations with the charge and current density described by (6) and (8), respectively. The relevant Maxwell's equations can be written as

$$\frac{d^2\phi}{dx^2} = \begin{cases} -4\pi e(N_i - N_e) & |x| \leq \ell_e \\ -4\pi e\, N_i & \ell_e < |x| \leq \ell_i \\ 0 & \ell_i < |x| \end{cases} \tag{9}$$

$$\frac{d^2A}{dx^2} = \begin{cases} -4\pi\frac{e}{c}\left[N_i\left(V_i - \frac{eA}{m_i c}\right) - N_e\left(V_e + \frac{eA}{m_e c}\right)\right] & |x| \leq \ell_e \\ -4\pi\frac{e}{c} N_i \left(V_i - \frac{eA}{m_i c}\right) & \ell_e < |x| \leq \ell_i \\ 0 & \ell_i < |x| \end{cases} \tag{10}$$

Note that $\ell_i > \ell_e$ has been assumed in (10) and (11) which can be expected for a current sheet in which electrons are the main carrier of the current. The boundary conditions for ϕ and A are:

$$\phi(x = 0) = A(x = 0) = 0$$

$$\left.\frac{d\phi}{dx}\right|_{x=0} = \left.\frac{dA}{dx}\right|_{x=0} = 0 \tag{11}$$

In addition to the boundary conditions, we impose an auxiliary condition to ensure that the electric field vanishes outside the boundary of the current sheet, i.e.,

$$\frac{d\phi}{dx} = 0 \qquad |x| \geq \max(\ell_e, \ell_i) \tag{12}$$

This condition requires that the net charge integrated across the current sheet must be zero. Since the number density in (6) is constant within the boundary of each species, the condition in (12) is equivalent to

$$N_e \ell_e = N_i \ell_i \tag{13}$$

It should be emphasized that (13) ensures charge neutrality outside but not inside the current sheet, unless $N_i = N_e$ and $\ell_i = \ell_e$. It can be shown from (7) that the necessary and sufficient condition for charge neutral solutions (i.e. charge neutrality inside and outside the current sheet) is given by

$$\frac{V_i}{V_e} = -\frac{\varepsilon_i}{\varepsilon_e} \tag{14}$$

Thus, the current sheet is non-neutral except when the ions and the electrons are streaming in opposite directions with their streaming speeds satisfying the relation in (14).

The solutions to (9) and (10) for ϕ and A are given by

$$\phi = 4\pi e N_e \begin{cases} \left(1 - \frac{N_i}{N_e}\right) \frac{x^2}{2} & |x| \le \ell_e \\ \left[\left(|x| - \frac{\ell_e}{2}\right) \ell_e - \frac{N_i}{N_e} \frac{x^2}{2}\right] & \ell_e < |x| \le \ell_i \\ \frac{\ell_e^2}{2} \left(\frac{N_e}{N_i} - 1\right) & \ell_i < |x| \end{cases} \tag{15}$$

$$A = \begin{cases} A_o \left[\cosh\left(\frac{x}{d_e}\right) - 1\right] & |x| \le \ell_e \\ A_o \left[\left(\frac{d_i}{d_e}\right) \sinh\left(\frac{\ell_e}{d_e}\right) \sinh \frac{(|x| - \ell_e)}{d_i} + \cosh\left(\frac{\ell_e}{d_e}\right) \cosh \frac{(|x| - \ell_e}{d_i}\right] & \\ - (A_o + A_i) \cosh \frac{(|x| - \ell_e)}{d_i} + A_i & \ell_e < |x| \le \ell_i \\ C_3 |x| + C_4 & \ell_i < |x| \end{cases} \tag{16}$$

where

$$A_o = \frac{N_e V_e - N_i V_i}{(eN_e/m_e c) + (eN_i/m_i c)} \tag{17}$$

$$A_i = m_i V_i c/e \tag{18}$$

$$d_e^2 = \frac{(m_e c^2/4\pi e^2 N_e)}{[1 + (m_e N_i/m_i N_e)]} \tag{19}$$

$$d_i^2 = m_i c^2/4\pi N_i e^2 \tag{20}$$

The constants C_3 and C_4 can be evaluated by matching the slope and the magnitude of A at $x = \ell_i$. Since the expressions for C_3 and C_4 are not required in (7) for determining the location of the boundary, they will not be given explicitly here.

The self-consistent electric and magnetic fields of the equilibrium current sheet are given by

$$\vec{E} = -4\pi e N_e \hat{x} \begin{cases} (1 - \frac{N_i}{N_e})\, x & |x| \leq \ell_e \\ (\pm \ell_e - \frac{N_i}{N_e}\, x) & \ell_e < |x| \leq \ell_i \\ 0 & \ell_i < |x| \end{cases} \tag{21}$$

$$\vec{B} = -\hat{y} \begin{cases} \frac{A_o}{d_e} \sinh\left(\frac{x}{d_e}\right) & |x| \leq \ell_e \\ \frac{A_o}{d_i}\left[\left(\frac{d_i}{d_e}\right) \sinh\left(\frac{\ell_e}{d_e}\right) \cosh\frac{(|x| - \ell_e)}{d_i} + \cosh\left(\frac{\ell_e}{d_e}\right) \sinh\frac{(|x| - \ell_e)}{d_i}\right] & \\ \quad - \frac{(A_o + A_i)}{d_i} \sinh\frac{(|x| - \ell_e)}{d_i} & \ell_e < |x| \leq \ell_i \\ \pm C_3 & \ell_i < |x| \end{cases} \tag{22}$$

where the "+" and "-" signs in $\vec{E}$ and $\vec{B}$ are for $x > 0$ and $x < 0$, respectively, and $\hat{x}$ and $\hat{y}$ are unit vectors. The magnitude of the electric field is maximum at $x = \pm \ell_e$ and is given by

$$E_{max} = 4\pi e N_e \left(1 - \frac{N_i}{N_e}\right) \ell_e \tag{23}$$

Now the only quantities to be determined are ℓ_e and ℓ_i which specify the electron and ion boundaries of the current sheet as defined by (7), i.e.,

$$\frac{\varepsilon_e + e\phi(\ell_e)}{\frac{1}{2}m_e V_e^2 \left[1 + eA(\ell_e)/m_e c V_e\right]^2} = 1 \tag{24}$$

$$\frac{\varepsilon_i - e\phi(\ell_i)}{\frac{1}{2}m_i V_i^2 \left[1 - eA(\ell_i)/m_i c V_i\right]^2} = 1 \tag{25}$$

These two simultaneous equations can be easily solved numerically after introducing the following dimensionless variables:

$$\phi^* = \frac{e\phi}{\varepsilon_{\perp i}} , \qquad A^* = \frac{eA}{\varepsilon_{\perp i}} , \qquad x^* = \frac{x}{D}$$

$$V_s^* = \frac{V_s}{V_{os}} , \quad \varepsilon_s^* = \varepsilon_s / m_e c^2 \tag{26}$$

where

$$\varepsilon_s = \varepsilon_{\perp s} + \tfrac{1}{2} m_s V_s^2$$

$$D^2 = \frac{\varepsilon_{\perp i}}{4\pi e^2 N_e} , \qquad V_{os}^2 = \frac{2\varepsilon_{\perp s}}{m_s} \tag{27}$$

Equations (24) and (25) can be rewritten, in terms of these dimensionless variables, as

$$\frac{1 + V_e^{*2} + (\varepsilon^*_{\perp i} / \varepsilon^*_{\perp e}) \phi^*(\ell_e)}{[V_e^* + (\varepsilon^*_{\perp i} / \varepsilon^*_{\perp e}) (\varepsilon^*_{\perp e} / 2)^{\frac{1}{2}} A^*(\ell_e)]^2} = 1 \tag{28}$$

$$\frac{1 + V_i^{*2} - \phi^*(\ell_i)}{[V_i^* - (m_e/m_i)^{\frac{1}{2}}(\varepsilon^*\ell_i/2)^{\frac{1}{2}}\lambda^*(\ell_i)]^2} = 1 \qquad (29)$$

The two unknowns in (28) and (29) are ℓ_e and ℓ_i. From (13) and (23), it is possible to express the unknown ℓ_i in terms of E_{max}. This is desirable because E_{max} is a quantity of primary interest while ℓ_i is not. The other unknown ℓ_e is also of practical interest since it gives the half-width of the current sheet.

Figure 1 shows the numerical solutions of (28) and (29) as functions of the electron streaming speed in units of the electron "thermal" speed. Figures 2 and 3 display the solutions as functions of the ion and electron "thermal" energies, respectively.

Note that the number density, N_e, in Figures 1 to 3 is the density of the current-carrying electron which is less than the total electron number density, N_t, in the presence of the background plasma.

The results shown in Figures 1 to 3 can be used to determine the width of the current sheet and the maximum electric field of the current sheet at any location provided the local plasma parameters of the current-carrying electron are known. The electron flux associated with the auroral field-aligned current is well known (Arnoldy, 1974; Anderson and Vondrak, 1975; Iijima and Potemra, 1978). However, the current velocity and the number density of the current-carrying electron are much less certain, especially at altitudes beyond a few thousand km.

Observations indicate that the field-aligned current at the auroral altitude ($\sim$ 100 km) is typically in the range of $j_{\parallel a} = 2 \times 10^{-6}$ A/m^2 ($\sim 10^9$ el/cm^2/sec) to $j_{\parallel a} = 2 \times 10^{-5}$ A/m^2 ($\sim 10^{10}$ el/cm^2/sec). If we take $j_{\parallel a} = 10^{10}$ el/cm^2/sec, the corresponding electron flux in the plasma sheet is given by

$$J_{\parallel p} = \frac{B_p}{B_a} j_{\parallel a} = \frac{10}{3 \times 10^4} \times 10^{10} \sim 3.3 \times 10^6 \text{ el/cm}^2\text{/sec} \qquad (30)$$

Assuming the current-carrying electrons are injected by a current source at the electron thermal speed, the number density of the injected electron in the plasma sheet is

$$N_{ep} = j_{\parallel p}/v_{oe} \cong 3 \times 10^{-3} \text{ cm}^{-3} \qquad (31)$$

which is much smaller than the total number density (~ 1 cm^{-3}) in the plasma sheet.

At 1 R_E altitude, the number density of the current-carrying electron is scaled by

$$N_e \text{ (1 } R_E) = \frac{B_1}{B_p} N_{ep} = 1 \text{ cm}^{-3} \qquad (32)$$

Assuming the proton thermal energy $\varepsilon_{\perp i} = 5$ keV and the electron $\varepsilon_{\perp e} =$ 0.5 keV, ℓ_e and E_{max} can be found from Figure 1; they are given by $\ell_e \cong 12$ km and $E_{max} \cong 0.98$ V/m. These predictions of the model are in reasonable agreement with observations reported by Mozer et al. (1977).

A general property of the solutions shown in Figures 1 to 3 is that the maximum potential difference across the current sheet is almost

equal to but slightly less than the ion "thermal" energy. This is a fundamental result which can be expected on the basis that the electrostatic potential in the current sheet is generated to confine the the ion in a high-β plasma.

We have shown in this section that the observed pair of perpendicular electric fields on auroral field lines can be identified as the inherent electric field of the auroral current sheet. It may be noted here that the proposed model is the first to relate self-consistently the auroral electric field and the auroral sheet current. The quantitative relationships shown in Figures 1 to 3 depend, to some extent, on the distribution function. However, qualitative behaviors of these relationships are characteristic of a non-neutral current sheet and are independent of the distribution function. For example, as the current velocity V_e increases, the width ℓ_e decreases and the maximum electric field E_{max} increases. It should be emphasized that the purpose of this paper is to point out the characteristics of non-neutral current sheet equilibria and to relate them to the auroral current sheet on a qualitative basis. The simple model presented in this section is used only to illustrate the physics of the non-neutral current sheet; its predictions should be viewed qualitatively rather than quantitatively.

It may be noted in passing that our simple current sheet model may be subject to the Kelvin-Helmholtz instability due to the presence of strong velocity shear in the beam as can be seen from (8). This instability may lead to the development of observable ripples on the boundary of the current sheet which are often associated with auroral arcs. It is possible that our non-neutral current sheet model is also unstable to

various types of current instabilities (Kindel and Kennel, 1971). However, it is unlikely that any of the instabilities is capable of disintegrating the electron sheet causing the auroral arc to break up.

3. Boundary Conditions and the Parallel Electric Field

The purpose of this section is to determine the upper and lower boundary conditions of the auroral acceleration region. The inherent electric field of the auroral current sheet can be treated as the upper boundary condition imposed on the acceleration region. The lower boundary condition can be determined as follows. We note first that E_x^m and $j_\parallel$ in Figure 4 are related through E_{max} and V_e shown in Figure 1. Because of the continuity of current, $j_\parallel$ should be connected to the ionospheric Pederson current J_p, by $\vec{\nabla} \cdot \vec{J}_p = j_\parallel$ or $J_p \cong j_\parallel L_i$ where L_i is approximately the half-width of the current sheet in the ionosphere. The electric field in the ionosphere E_x^i is determined by $E_x^i = J_p/\Sigma_p$ where Σ_p is the height integrated Pedersen conductivity. Thus, for a given $j_\parallel$ the ionosphere determines its own electric field. If $E_x^m > E_x^i$, the potential contour lines should be shaped like the letter V and thus an upward parallel electric field $E_\parallel$ is forced to appear along field lines in the current sheet.

For an estimate of E_x^m and E_x^i, we use the same set of values considered in the previous section, i.e. $\varepsilon_{\perp i} = 5$ keV, $\varepsilon_{\perp e} = 0.5$ keV, $V_e = v_{oe}$, $V_i = 0$ and $N_e = 1$ cm^{-3} at 1 R_E. We have $\ell_e \cong 12$ km, $E_{max} = 0.98$ V/m at 1 R_E altitude, $j_\parallel \cong 2 \times 10^{-5}$ A/m^2; note that the above value of $j_\parallel$ is within the range of observed values by rockets and satellites in connection with discrete auroras. Assuming $L_i \cong \ell_e$ and $\Sigma_p \cong 1$ mho (pre-arc) to 10

mho (arc), then $J_p \cong 2 \times 10^{-2}$ A/m and $E_x^i \cong 20$ mV/m (pre-arc) to 2 mV/m (arc). Thus E_x^m ($\cong$ 2500 mV/m)>> E_x^i ($\cong$ 20 mV/m). This shows that almost the entire potential difference associated with the inherent field of the current sheet is dropped along the auroral field lines between the upper and the lower boundaries resulting in an upward directed parallel electric field component.

It may be noted here that the presence of parallel electric field in a collisionless plasma does not necessarily imply the presence of anomalous resistivity in the sense of a local relationship between the electric current density and the electric field (e.g. Fälthammar, 1977). The double layer and the electrostatic shock solutions are examples of parallel electric field without requiring the presence of anomalous resistivity. In any case, the main point of this section is to show the necessity of field-aligned potential drop due to the boundary condition on $E_\perp$ in the ionosphere regardless how the potential drop is maintained. The question of whether the parallel electric field is maintained primarily by the anomalous resistivity or the double layer or the electrostatic shock remains somewhat controversial at present. A discussion of this topic can be found in Fälthammar (1977) and Shawhen et al., (1978).

4. Prediction of the Model and Some Supporting Observations

The proposed theory can make several predictions even in its early development stage. This is because most of the observable effects are determined by the upper and/or lower boundary conditions, rather than conditions in the intermediate regions.

(i) The theory predicts that the maximum electric field (E_{max}) and the width of the current sheet ($2\ell_e$) are anti-correlated.

Although the predicted relation could directly be determined by a future study of satellite data, it has been known that the brightness of an auroral arc is anti-correlated with its width. Maggs and Davis (1968) found on the basis of the TV study that all types of auroral arcs exhibit a strong tendency to become thinner as their brightness increases. We may consider this observation to be an indirect support of the prediction.

(ii) The theory predicts that the peak energy of auroral electron flux increases toward the equatorial boundary of the oval of discrete auroras.

This prediction is based on the fact that E_{max} is proportional to the thermal energy of protons in the plasma sheet. It has been shown by Hones (1972) that the average energy of protons in the plasma sheet decreases significantly from the midplane of the plasma sheet to the boundary. On the basis of a geometrical consideration of the magnetic configuration, we would expect that the peak energy of auroral electrons increases toward the equatorial boundary of the oval. Burch (1968) and McDiarmid et al. (1975) have already shown this tendency by their direct measurements of auroral electrons. Eather (1969) showed the same tendency on the basis of their photometric study of auroral emissions.

5. Conclusion

(i) We have identified the pair of the perpendicular electric fields with the inherent electric field of the auroral current sheet.

(ii) We have shown that almost the entire potential difference associated with the inherent electric field of the current sheet is dropped along the auroral field lines between the upper (the plasma sheet) and lower (the ionosphere) boundaries. As a result, there should be an upward electric field in the auroral current sheet.

(iii) The maximum intensity of the pair of the electric fields and the width of the auroral current sheet are self-consistently determined by providing only the intensity of the field-aligned density and the thermal energy of electrons and protons in the plasma sheet.

(iv) A few predicted relationships among the current sheet parameters have direct or indirect observational supports.

(v) Above all, we feel that the proposed theory self-consistently relates, for the first time, the auroral electric field and the auroral sheet current.

Acknowledgment: This work was supported in part by Air Force Geophysics Laboratory, Air Force Systems Command under Contract F 19628-77-C-0038 and by the Atmospheric Sciences Section of the National Science Foundation under Grants ATM 77-11371 and ATM 74-23823 to the University of Alaska.

References

Alfvén, H., Electric currents in cosmic plasmas, Rev. Geophys. Space Phys., 15, 271, 1977.

Anderson, H.R. and R.R. Vondrak, Observations of Birkeland current at auroral altitude, Rev. Geophys. and Space Phys., 13, 243, 1975.

Arnoldy, R.L., Auroral particle precipitation and Birkeland current, Rev. Geophys. Space Phys., 12, 217, 1974.

Block, L.P., Potential double layers in the ionosphere, Cosmic Electrodynamics, 3, 349, 1972.

Block, L.P., Double layers, Physics of the Hot Plasma in the Magnetosphere, p. 229, ed. by B. Hultqvist and L. Stenflo, Plenum Press, New York, 1975.

Burch, L., Low-energy electron fluxes at latitudes above the auroral zone, J. Geophys. Res., 73, 3585, 1968.

Burch, J.L., W. Lennartsson, W.B. Hanson, R.A. Heels, J.H. Hoffman and R.A. Hoffman, Properties of spikelike shear flow reversals observed in the auroral plasma by atmosphere explorer C, J. Geophys. Res., 81, 3886, 1976.

Davis, T.N., Observed characteristics of auroral arcs, Space Science Reviews, (submitted) 1978.

Eather, R.H., Latitudinal distribution of auroral and airglow emissions: The soft auroral zone, J. Geophys. Res., 74, 153, 1969.

Fälthammar, C.-G., Problems related to macroscopic electric fields in the magnetosphere, Rev. Geophys. Space Phys., 15, 457, 1977.

Hammer, D.A. and G. Rostoker, Propagation of high current relativistic electron beams, Phys. Fluids, 13, 1831, 1970.

Hones, E.W. Jr., Review and interpretation of particle measurements made by the Vela satellites in the magnetotail, Physics of the Magnetosphere, p. 392, ed. by R. Carovillano, J.F. McClay and H.R. Rodoski, D. Reidel Pub. Co, Dordrecht-Holland, 1968.

Hudson, M.K., R.L. Lysak and F.S. Mozer, Magnetic field-aligned potential drops due to electrostatic ion cyclotron turbulence, Geophys. Res. Lett., 5, 143, 1978.

Iijima, T. and T.A. Potemra, Large-scale characteristics of field-aligned current associated with substorms, J. Geophys. Res., 83, 599, 1978.

Kan, J.R. and H.-M. Lai, Highly force-free relativistic electron beam equilibrium, Phys. Fluids, 15, 2041, 1972.

Kan, J.R. Energization of auroral electrons by electrostatic shock waves, J. Geophys. Res. 80, 2089, 1975.

Kan, J.R., and S.-I. Akasofu, Energy source and mechanisms for accelerating the electrons and driving the field-aligned currents of the discrete auroral arc, J. Geophys. Res., 81, 5123, 1976.

Kindel, J.M. and C.F. Kennel, Topside current instabilities, J. Geophys. Res., 76, 3055, 1971.

Longmire, C.L., Elementary Plasma Physics, Interscience Publishers, 1963.

Maggs, J.E. and T.N. Davis, Measurements of the thickness of auroral structures, Planet. Space Sci., 16, 205, 1968.

McDiarmid, J.B., J.R. Barrows and E.E. Budzinski, Average characteristics of magnetospheric electrons (150 eV to 200 keV) at 1400 km, J. Geophys. Res., 80, 73, 1975.

Mozer, F.S., C.W. Carlson, M.K. Hudson, R.B. Torbert, B. Parody, J. Yatteau, and M.C. Kelley, Observations of paired electrostatic shocks in the polar magnetosphere, Phys. Rev. Lett., 38, 292, 1977.

Papadopoulos, K., A review of anomalous resistivity for the ionosphere, Rev. Geophys. Space Phys., 15, 113, 1977.

Shawhan, S.D., C.-G. Fälthammar and L.P. Block. On the nature of large auroral zone electric fields at 1 R_E altitude, J. Geophys. Res., 83, 1049, 1978.

Swift, D.W., An equipotential model of auroral arcs, 2. Numerical solutions, J. Geophys. Res., 81, 3935, 1976.

Wescott, E.M., H.C. Stenbaek-Nielsen, T.J. Hallinan, T.N. Davis and H.M. Peek, The skylab barium plasma injection experiments, 2. Evidence for a double layer, J. Geophys. Res., 81, 4495, 1976.

Figure Captions

Figure 1 — The half width of the current sheet (ℓ_e) and the maximum perpendicular electric field of the current sheet (E_{max}) are plotted as functions of the electron streaming speed (V_e) for $\varepsilon_{\perp i}$ = 5 keV, $\varepsilon_{\perp e}$ = 0.5 keV and V_i = 0. Note that N_e is the electron number density of the current sheet.

Figure 2 — The half width of the current sheet (ℓ_e) and the maximum perpendicular electric field of the current sheet (E_{max}) are plotted as functions of the ion 'thermal' energy ($\varepsilon_{\perp i}$) for $\varepsilon_{\perp e}$) = 0.5 keV, $V_e = v_{oe}$ and V_i = 0. Note that N_e is the electron number density of the current sheet.

Figure 3 — The half width of the current sheet (ℓ_e) and the maximum perpendicular electric field of the current sheet (E_{max}) are plotted as functions of the electron 'thermal' energy ($\varepsilon_{\perp e}$) for $\varepsilon_{\perp i}$ = 5 keV, $V_e = v_{oe}$ and V_i = 0. Note that N_e is the electron number density of the current sheet.

Figure 4 — A schematic diagram illustrating the relative location of the upper boundary condition (E_x^m), the lower boundary condition (E_x^i) and the distribution of $E_{\parallel}$ along field lines in the current sheet.

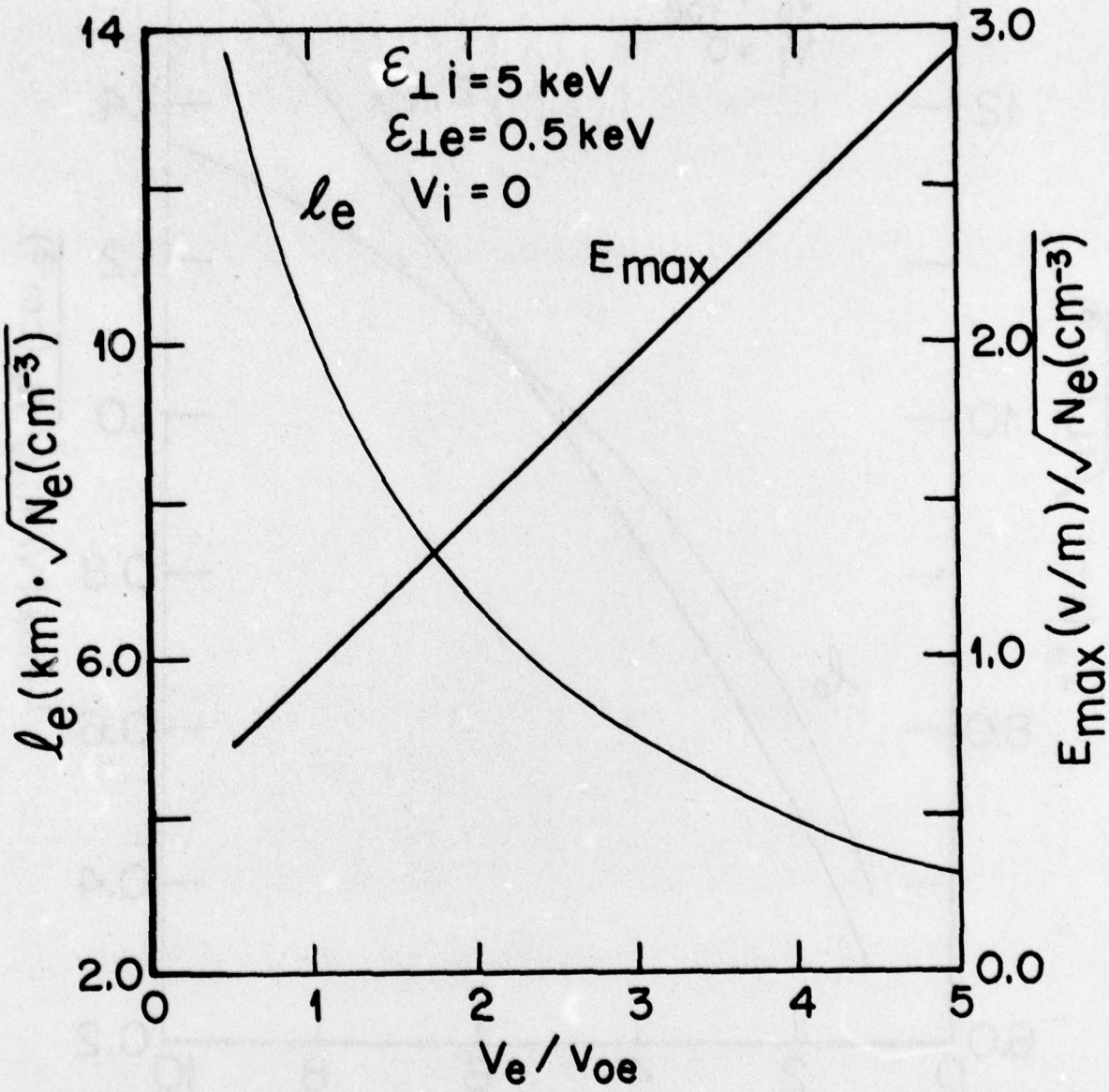
$\mathcal{E}_{\perp i}$ = 5 keV
$\mathcal{E}_{\perp e}$ = 0.5 keV
$V_i = 0$
ℓ_e
E_{max}
ℓ_e(km) · $\sqrt{N_e(cm^{-3})}$
E_{max} (v/m) / $\sqrt{N_e(cm^{-3})}$
14
10
6.0
2.0
3.0
2.0
1.0
0.0
0
1
2
3
4
5
V_e / V_{oe}

Fig 1

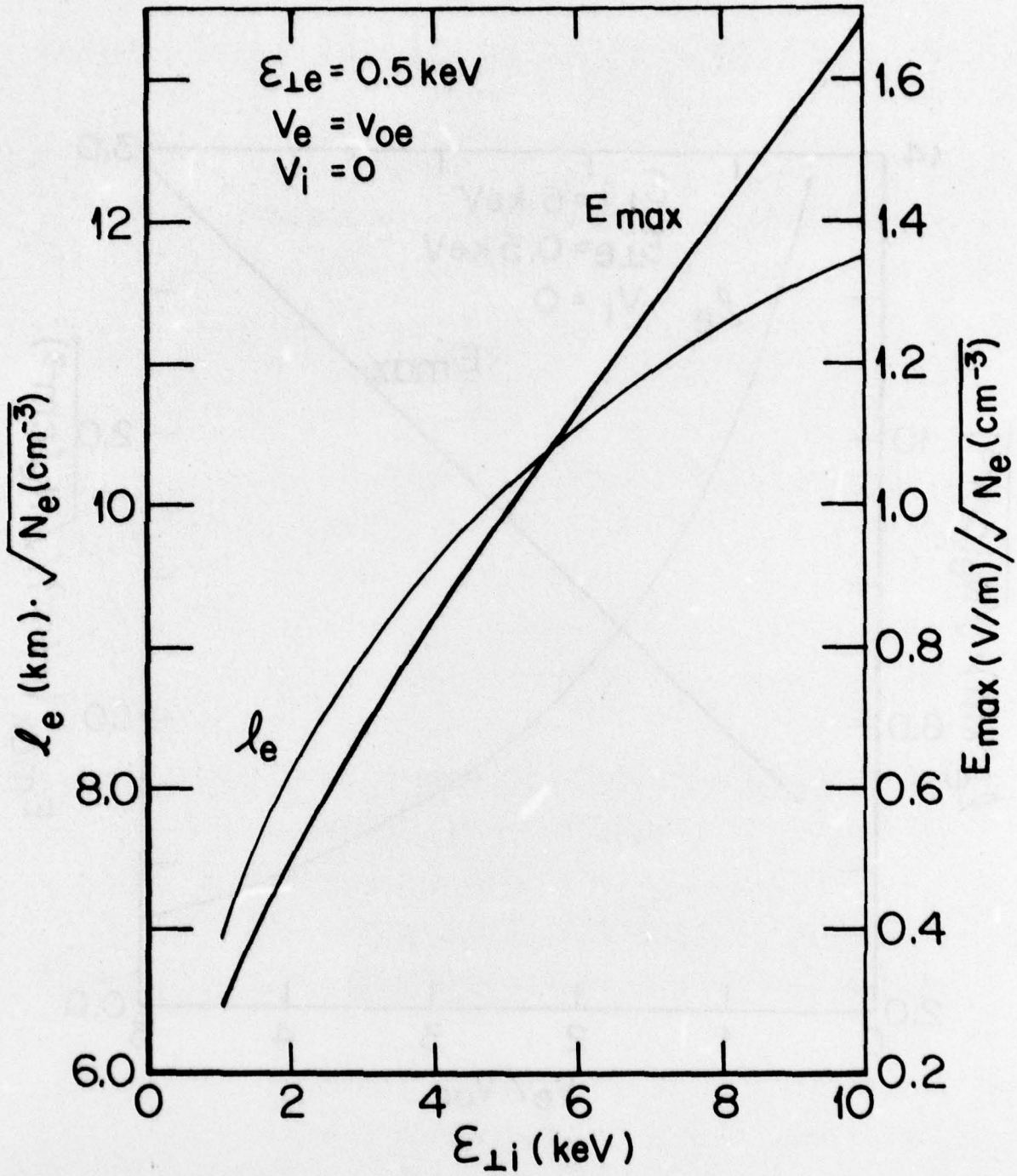
$\mathcal{E}_{\perp e}$ = 0.5 keV
$V_e = V_{oe}$
$V_i = 0$
E max
ℓ_e
ℓ_e (km) · $\sqrt{N_e(cm^{-3})}$
E_{max} (V/m) / $\sqrt{N_e(cm^{-3})}$
$\mathcal{E}_{\perp i}$ (keV)
12
10
8.0
6.0
1.6
1.4
1.2
1.0
0.8
0.6
0.4
0.2
0
2
4
6
8
10

Fig 2

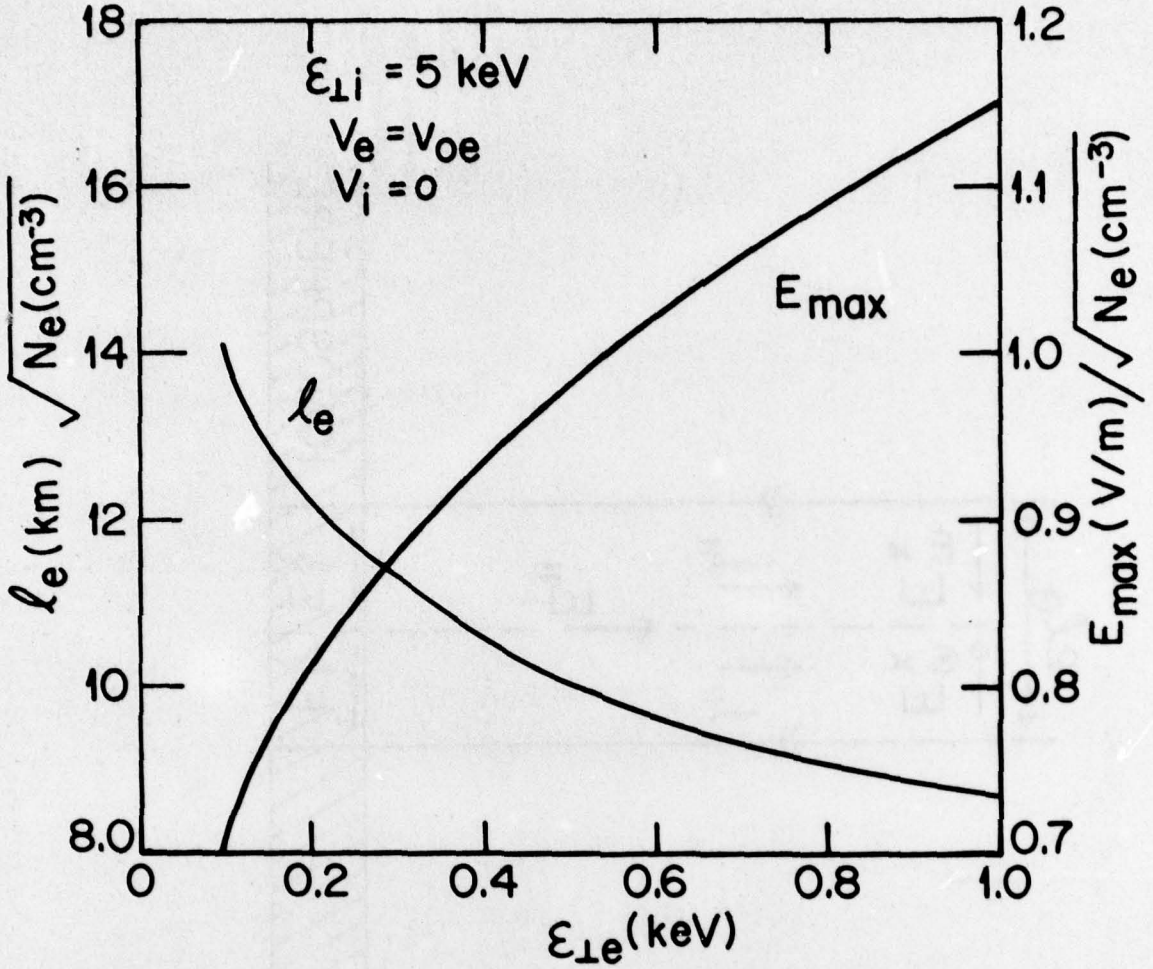
$\mathcal{E}_{\perp i}$ = 5 keV
$V_e = V_{oe}$
$V_i = 0$
E_{max}
ℓ_e
ℓ_e (km) $\sqrt{N_e(cm^{-3})}$
E_{max} (V/m) $/\sqrt{N_e(cm^{-3})}$
$\mathcal{E}_{\perp e}$ (keV)
18
16
14
12
10
8.0
1.2
1.1
1.0
0.9
0.8
0.7
0
0.2
0.4
0.6
0.8
1.0

Fig 3

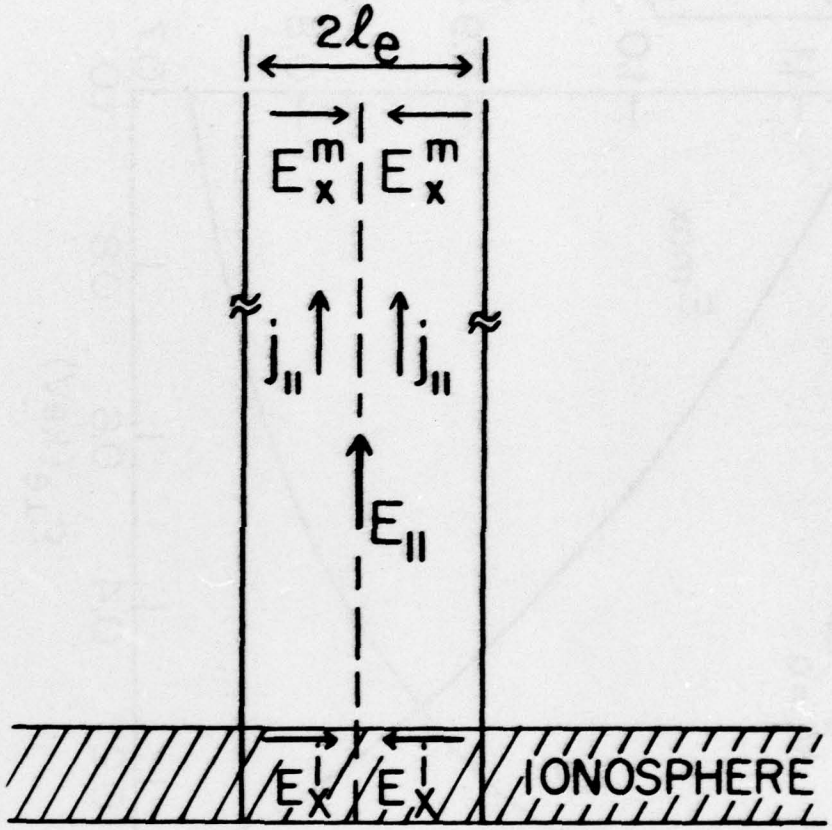
$2\ell_e$
E_x^m
E_x^m
$j_{\parallel}$
$j_{\parallel}$
$E_{\parallel}$
E_x^i
E_x^i
IONOSPHERE

Fig 4